EFFECTS OF FUNCTIONALIZED NANOSILICA WITH LOW AMINOSILANE CONTENT ON THE MECHANICAL PROPERTIES AND MICROSTRUCTURE OF CEMENTITIOUS MATERIALS

Andréia de Paula[1]*; Yuri Sotero Bomfim Fraga[2] *; João Henrique da Silva Rêgo[3]; Maria José de Souza Serafim[4]

[1] University of Brasília - UnB, 70910-900, Brasília, DF.
paula_adp@yahoo.com.br
[2] Federal University of Acre – UFAC, 69920-900, Rio Branco, AC.
yurisotero.engcivil@gmail.com
[3] University of Brasília - UnB, 70910-900, Brasília, DF.
jhenriquerego@unb.br
[4] University of Brasília - UnB, 70910-900, Brasília, DF.
mariajss19@yahoo.com.br

ABSTRACT

To investigate the effect of functionalizing NS with low levels of APTES on the mechanical and microstructural properties of cementitious materials, four pastes were examined: one produced with Portland cement (REF); another with 1% substitution of cement with nanosilica (NS); another with 1% substitution of cement with APTES-functionalized nanosilica using 2mL of APTES (NSFA2); and one with 1% substitution of cement with APTES-functionalized nanosilica using 4mL of APTES (NSFA4). Compressive strength at 1, 3, 7, and 28 days of hydration, as well as porosity measured by mercury intrusion porosimetry (MIP), were evaluated in the cementitious mixtures. The compressive strength of the NSFs was higher than that of REF and NS. NSFA4 achieved a 28% higher strength compared to REF and 17% higher strength compared to NS at 28 days. MIP showed that the additions of NS and NSF resulted in a decrease in total porosity compared to the reference mortar.

KEYWORDS: *portland cement; nanosilica (ns); functionalization; functionalized nanosilica (nsf).*

I. INTRODUCTION

Several studies have demonstrated that cementitious materials with silica nanoparticles (NS) exhibit an increase in mechanical strength, especially at early ages, when compared to pure cement [[1]; [2]; [3], [4]; [5]; [6]], due to the high pozzolanic reactivity and accelerating effect on cement hydration exhibited by NS [[7]; [8]].

Due to its much smaller particle size compared to cement, NS tends to be effective in filling the voids between cement grains, increasing the packing density of cementitious materials, which improves their strength and durability [[9]; [7]; [10]; [1]]. According to Singh *et al*. [11] and Schmalz [12], in the presence of NS, pozzolanic reactions and nucleation reactions occur during cement hydration, resulting in the formation of additional C-S-H that favors the early hydration of cement. For Gu *et al*. [13] and Fang *et al*. [14], the formation of pozzolanic C-H-S improves the microstructure of the paste by filling the interparticle spaces, leading to denser packing and reducing the need for water, improving the mechanical properties and durability of concretes and mortars. In their research, Singh et al. (2011) observed that the CH content in the cement paste with incorporated NS was lower compared to the reference paste, concluding that the addition of a small amount of NS significantly improves the morphology and mineralogy of cementitious materials.

However, the incorporation of NS in cementitious matrix also poses some challenges to be overcome. Agglomeration of NS, due to inadequate dispersion, results in negative effects on the rheological behavior, workability, and final hardened properties of cement composites [[16]; [17]]. The limitation of workability of pastes and mortars can lead to possible problems in long-term durability and strength [[18]; [19]; [20]; [21]]. Another issue with the use of NS is its extreme reactivity in the early ages, which may lead to the formation of a layer of C-S-H on the surface of clinker grains and hinder the complete hydration of this material and, consequently, its rate of compressive strength gain at 28 days [[22]; [11]; [23]; [13]; [24]; [25]; [26]; [2]; [27]; [17]; [28]; [6]]. This effect justifies the decrease in the difference in compressive strength of cementitious materials with NS compared to reference cementitious materials (only with cement) as the hydration age increases. The compressive strength results obtained by Martins [5] show that although NS provides mechanical performance gains in the early ages, at 28 days, this initial gain does not have the same effect due to autogenous shrinkage and the formation of the C-S-H layer on the clinker surface, as also observed by other authors. [[24]; [29]; [30]; [4]].

In order to overcome the challenges of using NS in cementitious materials, some researchers began to promote changes in the NS surface (a process called functionalization) to create adaptations in the material [[31]; [32]; [33]; [34]; [35]; [36]; [37]; [38]] and include new chemicals functions to nanoparticle [[29]; [5]]. In the case of NS, the chemical reaction that occurs during functionalization replaces the silanol groups (OH) on the surface of the NS by another group of greater interest, usually the amine groups, normally using the reagent 3-aminopropyltriethoxysilane (APTES). Amine groups are polymers that have a good connection with the NS surface and are used in various isolated functionalization processes and in functionalization processes with other components [[4]; [13]].

Studies indicate that the functionalization of NS with aminosilanes forming nanosilica functionalized with aminosilanes (NSF), increases its affinity to connect to other chemical additives, such as shrinkage reducing additive (SRA) and polycarboxylate ether superplasticizers (PCE) ([34], [37]; [35]]. According to Collodetti *et al*. [31], Vasconcellos *et al*. [40] and Fraga *et al*. [29] the hydration kinetics of cement pastes is altered with the incorporation of NSF when compared with a reference paste containing only cement or with a paste containing NS. The effects vary according to the chemical group used, however, in general, there is a delay in cement hydration. Studies with NSF with aminosilanes show an improvement in the dispersion of the material, avoiding agglomeration which can lead to an acceleration in cement hydration and the filling of internal voids in the cementitious matrix, making the microstructure of composites more compact and improving compressive strength [[3]; [13]]. Vasconcellos *et al*. [6] found that the pastes containing NSF exhibited delayed hydration, reduced additive demand, formation of additional C-S-H, densifying the microstructure of cement pastes, improved cementitious matrix and workability, a reduction in total pore volume and a contribution to the mechanical performance of cementitious matrices at advanced ages. Martins [5] verified that the variation in the proportion of NS functionalizations with aminosilanes causes alterations in the hydration kinetics, in the formation of C-S-H, in the pore size distribution and in the compressive strength of Portland cement pastes and also found a delay in the induction time, as also observed by Vasconcellos [4] and Vasconcellos *et al*. [6].

The results of these studies demonstrate that the higher the content of APTES in the NS, the greater the delay in the hydration reactions of the pastes. According to Collodetti *et al*. [31], amorphous silica has a maximum concentration of OH groups on its surface that are apt to be replaced by other organic groups. Thus, there is a maximum percentage of functional groups that can be grafted onto its surface, reaching a saturation degree. Therefore, the APTES content on the NS may influence the effect of the NS on cementitious materials, making it important to further study the effect of reducing the APTES content of the NS with aminosilane on the mechanical and microstructural properties of cementitious materials.

This article has been divided into 4 sections. The first section deals with the introduction to the studied topic. The second section addressed the experimental program that was developed to achieve the objectives. The experimental program was divided into 4 stages: Stage 1: Materials. Stage 2: Functionalization of NS. Stage 3: Preparation of Pastes. Stage 4: Tests for the analysis of pastes and mortars. The third section presents the experimental results obtained with analysis and discussions of the data. The presentation of results and discussions follows the order of the stages developed in the

experimental program. The fourth section presents the conclusions drawn based on the experimental results. Finally, the references used to support this article are provided.

II. EXPERIMENTAL PROGRAM

2.1 MATERIALS

For the development of the experimental program, the following materials were used: Portland cement CP-V ARI, following the Brazilian technical standard [41], equivalent to type III ASTM C150 and CEM I EN 197, due to the low content of additions; colloidal nanosilica (NS) prepared in an aqueous suspension of 30% by weight NS; superplasticizer additive (SP) type 2 according to the Brazilian technical standard [42]; 3-Aminopropyltriethoxysilane reagent (APTES) 99% pure; dichloromethane 99.8% PA ACS used as solvent; deionized water supplied by the MiliQ system - Millipore equipment (Chemistry Institute - UnB) and water from the public supply system in Brasilia.

Table 1 presents the physical and mechanical properties of Portland cement CP V-ARI, NS, APTES, dichloromethane and SP additive. The chemical analysis of Portland cement CP V-ARI and NS was obtained by X-ray fluorescence spectrometry (FRX).

Table 1 - Properties of CP V-ARI, NS, APTES, dichloromethane and SP additive.

Material	Properties		Results	Material	Properties		Results
Portland cement CP V-ARI	Setup time: initial (h:min)		02:41	NS	Specific mass (g/cm³)		1.20
	Setting time: final (h:min)		03:11		pH		10,707
	Residue on sieve nº 200 (%)		4,26		Solid content (%)		32,5
	Blaine Specific Area (cm²/g)		4692		Average diameter (nm)		8,284
	Specific mass (g/cm³)		3,06		Compounds (%)	SiO2	100
	Compressive strength (MPa)	1 day	19,93			Cr	0,004
		3 days	31,4			K2O	0,02
		7 days	38,55			Cu	0,001
	D10 (µm)		1,89			S	0,183
	D50 (µm)		14,19			CaO	0,008
	D90 (µm)		33,59			Zr	0,005
	Average Diameter (µm)		16,37			Au	0,002
	Compounds (%)	SiO2	25,22			Th	0,001
		Al2O3	7,72	APTES	Color		Colorless
		Fe2O3	3,46		Form		liquidate
		CaO	55,58		Color test		< 10 APHA
		K2O	1,06		Purity (%)		99,6
		TiO2	0,42		Molar weight (g/mol)		221,37
		P2O5	0,24	SP	Specific mass (g/cm³)		1.095
		MnO	0,11		pH		3.8
		SO3	6,19		Solid content (%)		40

In the X-ray diffraction (XRD) test, we aimed to identify the crystalline or amorphous phases of the cement. The tests were performed using a RIGAKU brand Ultima IV diffractometer according to the parameters of 2 theta: 2 to 60°, step: 0.05°, speed: 5°/min. The diffractogram of the cement sample is

presented in Figure 1 (a). In the diffractogram, anhydrous calcium silicate minerals (C_2S and C_3S) and anhydrous calcium iron-aluminate (C_4AF) were identified, confirming the chemical composition of the respective type of cement. The NS and NSF samples were also analyzed using the XRD test. The diffractogram of the colloidal NS sample is presented in Figure 1 (b). The diffractograms of the NSF's followed the same pattern as the NS colloidal, only presenting peak intensities at 2 theta = 10° and 2 theta = 23° with different intensities.

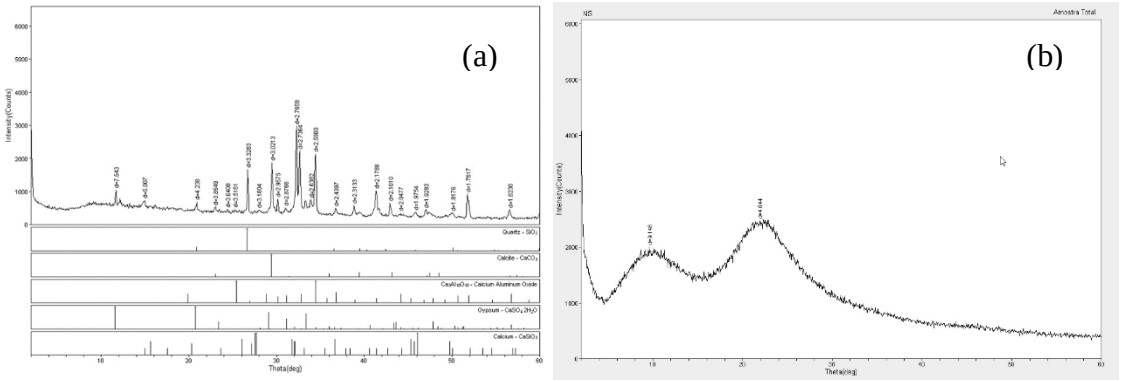

Figure 1 - Diffractogram of Portland Cement CPV -ARI and NS colloidal

2.2 FUNCTIONALIZATION OF THE NS

The NS functionalization procedure with APTES took place at room temperature using a round bottom flask coupled to a condenser to avoid loss of reagents by evaporation. This set was taken inside the hood. The dichloromethane and colloidal NS were added to the flask and magnetic stirring was carried out at a speed of 900 rpm. Then, APTES was added in the chosen volumetric proportions (2 and 4mL) and the stirring speed was changed to 1500 rpm. At the exact moment when APTES came into contact with dichloromethane and colloidal NS, the reaction start time was recorded, and the materials were stirred for 24 hours at room temperature.

After 24 hours, with the end of the stirring period, the mixture was transferred to a separatory funnel, where the formation of a two-phase system could be observed. After separating the phases, the organic phase, with a transparent color (which is dichloromethane), was collected and stored for later disposal. The phase containing NSF was mixed with deionized water and taken to the Cole Parmer ultrasonic processor to sonicate for 10 minutes, at an amplitude of 65%, with the device remaining at rest for 10s every 50s. Finally, the samples were collected and stored in glass bottles for subsequent performance of characterization tests in order to evaluate the effectiveness of the functionalization process. It was also necessary to check the pH of the NS and NSF's and carry out the solids content test of the samples since the amount of water in the samples was deducted from the mixing water of the pastes and mortars. The pH and solids content results are shown in Table 2.

Table 2 – Results of the Solid Content and pH tests of the colloidal NS and the NSF's.

Sample	Solid Content (%)	pH
NS	32,5	10,71
NSFA2	14	11,06
NSFA4	14,5	11,30

2.2.1 NS and NSF characterization tests

To confirm that the APTES silanes were grafted onto the NS nanoparticles and to evaluate the properties of the new NSF surface, dynamic light scattering (DLS), transmission electron microscopy (TEM) and thermogravimetric analysis (TGA) tests were performed. To carry out these tests, the NSF samples were

dried in the open air in a Petri dish. After drying, they were finely crushed with the aid of an agate mortar and pestle and stored in containers until the date of the tests.

The Dynamic Light Scattering (DLS) technique was used to verify the increase in the hydrodynamic radius of silica nanoparticles caused by functionalization. We sought to verify whether there was evidence of an increase in particle size with functionalization, a technique performed by other researchers with NSF [[34]; [13]; [43]; [2]; [44]; [27]]. The DLS assay was made using the Zetasizer Nano Series apparatus. To carry out the test, samples of colloidal NS and NSF were inserted into the cell type PC51115 (Glass cuvette with square aperture).

According to Vasconcellos [4], the Transmission Electron Microscopy (TEM) technique is performed on the NS and NSF dispersions, in order to evaluate the morphology, degree of dispersion, aggregation and dimensions of the particles. The samples were dispersed in aqueous media using the ultrasonic cleaner. An aliquot of the sample was deposited on the copper grid (specifications: 400 mesh copper coated copper grid). After drying, the samples were analyzed in the Transmission Electron Microscope (TEM), JEM-2100, Jeol, Tokyo, Japan, equipped with EDS, Thermo Scientific, operating at 200kV.

Thermal analyzes were performed on the NS and NSFA samples, in order to obtain the mass loss variation as a function of the increase in temperature at a programmed rate, seeking to compare them with the reference sample. Through this test, it was possible to evaluate the functionalization of the NS through the loss of mass of the samples as a function of the increase in temperature. Thermal analyzes were performed on solid samples in a thermogravimetric analyzer from SHIMADZU, model DTG-60H. The test took place under a nitrogen gas flow of 50 mL /min, at a heating rate of 10 °C/min from room temperature to 1000 °C. The assay was performed using platinum crucibles.

2.3 PREPARATION OF PASTES AND MORTARS

For conducting the Mercury Intrusion Porosimetry (MIP) tests at 28 days, five different cement paste mixtures were prepared as shown in Table 2. All pastes were produced with a water-to-binder ratio (w/b) of 0.35. In this research, certain parameters were fixed for paste production in order to reduce the number of variables. The fixed parameters were: Curing condition: curing in water saturated with lime, as per [45]; Consistency for pastes (110±10mm) referenced in the study by Vasconcellos [4].

Table 3 – Nomenclature and composition of pastes

Cement paste	Abbreviation	Cement (g)	Water (g)	NS (g)	NSF2 (g)	NSF4 (g)	Additive SP (%)	Spread (mm)
100% CP V	P-REF	2000	691,3	-	-	-	0,6	119,28
99% CP V + 1% NS	P-NS	1980	643,96	61,54	-	-	1	112,79
99% CP V + 1% NSFA2	P-NSFA2	1980	564,09	-	142,86	-	0,9	115,04
99% CP V + 1% NSFA4	P-NSFA4	1980	569,02	-	-	137,93	0,9	113,70

In the preparation of the pastes, the superplasticizer (SP) additive content used had a variation from one paste to another, so that all had a spreading of 110±10mm, in the mini-slump test. To keep the exact a/ agl ratio, the amount of water from the NS in aqueous suspension, from the NSF's and from the SP additive was deducted from the mixing water, for this purpose, according to the previously determined solids content. The pH of the NSF's was checked using a pH meter. The process of preparing the pastes followed the recommendations of [46], with some adaptations in the mixing time and in the loading sequence of the materials.

In order to carry out the compressive strength test at 1, 3, 7 and 28 days, five different traces of cement mortar were molded, according to Table 4, as was the case with the pastes. All mortars were produced in relation to a/ agl = 0.35. The same replacement levels of Portland and NS cement used to make the pastes and the same SP additive content found in the production of cement pastes were maintained.

Table 4 – Nomenclature and composition of mortars

Cement paste	Abbreviation	Cement (g)	Water (g)	Normal sand in 4 fractions (g)	NS (g)	NSF2 (g)	NSF4 (g)	Additive SP (%)	Spread (mm)
100% CP V	A-REF	700	241,9	335 x 4	-	-	-	0,6	189,50
99% CP V + 1% NS	A-NS	693	207,345	335 x 4	48,27	-	-	1	163,50
99% CP V + 1% NSFA2	A-NSFA2	693	197,46	335 x 4	-	49,966	-	0,9	183,51
99% CP V + 1% NSFA4	A-NSFA4	693	199,114	335 x 4	-	-	48,27	0,9	184,67

The molding of four specimens of mortar with 50 mm in diameter and 100 mm in height was carried out, according to [45]. The spreading of the mortars was obtained by testing the consistency table. The mixing of mortars was made in a planetary mixer and will follow the procedures described in the literature, with adaptations [[47]; [48]].

2.4 TESTS FOR ANALYSIS OF PASTES AND MORTARS

To verify the mechanical properties of cement mortars using NSF, compressive strength tests were carried out at 1, 3, 7 and 28 days of hydration. The cylindrical specimens with 50 mm in diameter and 100 mm in height for the compressive strength test were molded following [45]. After molding, the specimens were taken to the humid chamber where they remained for 24 hours. Then, the specimens were demoulded and taken to cure submerged in a solution of water and lime to avoid calcium leaching, where they remained until the specified date for rupture (1, 3, 7 and 28 days). On the date of failure, the specimens were subjected to compressive stress, until failure, in the Denison Press model TIA / MC with a capacity of 200,000 kg. The adopted resistance was the average of the individual resistances of the 4 specimens of the same age, as recommended by [45].

Mercury intrusion porosimetry (MIP) tests were conducted on the pastes to assess the microstructure of cementitious materials. The samples were submerged in isopropanol for 24 hours to halt hydration, following the methodology proposed by Scrivener et al. (2016) and Alonso-Domínguez et al. (2017), with adaptations regarding the immersion time in isopropanol. After this period, the samples were dried in a 40°C oven for 24 hours to ensure complete removal of isopropanol. Subsequently, the samples were stored in containers containing silica gel and welded lime until the date of the microstructural tests. The samples for the MIP tests were cut into approximately 1 cm cubic pieces using a circular saw. This test aims to evaluate the porous structure of cementitious pastes after 28 days of hydration. The test parameters included mercury with a surface tension of 0.485 N/m, density of 13.5335 g/mL, and contact angle of 130°C. The pressure range used in the test was approximately 0.6582 psi to 25.4162 psi. The equipment used was the Micromeritics Poresizer, model 9320. Based on this test, the pores were quantified according to their sizes.

III. RESULTS AND DISCUSSIONS

3.1 CHARACTERIZATION OF NS AND NSF'S

Analyzes regarding the characterization of NS and NSF are essential for understanding their influence on the microstructure of cement pastes. In this item, the results and discussions of the microstructural analyzes carried out for the characterization of the NS and NSF's are presented, in order to evaluate the behavior in terms of structure, morphology and composition, through the Dynamic Light Scattering (DLS) and Thermogravimetric Analysis (TGA). Figure 2 presents the graphs of the Dynamic Light Scattering (DLS) results of the NS and the NSF's. Table 5 summarizes the values of the hydrodynamic radius of the NS and the NSF's.

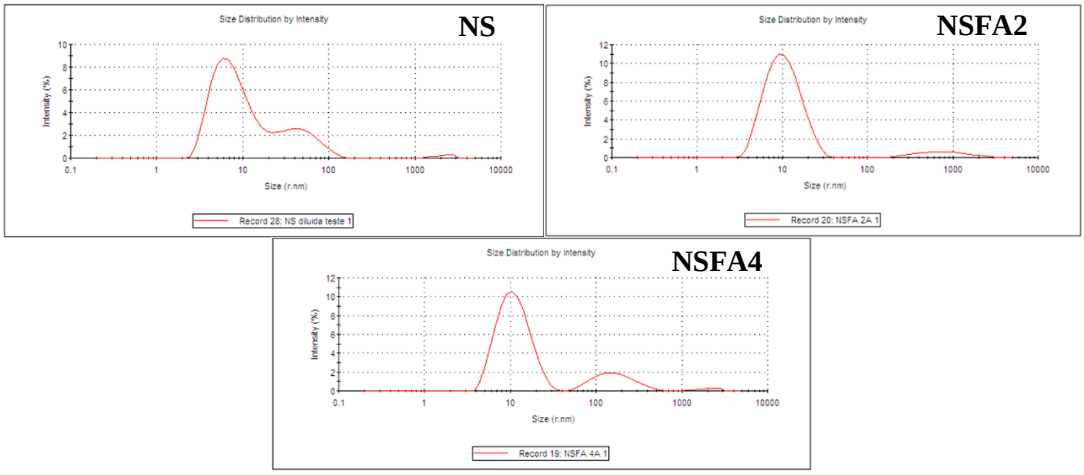

Figure 2 – Results of Dynamic Light Scattering (DLS) of NS, NSFA2 and NSFA4

Table 5 - Values of the hydrodynamic radius of the samples

Sample	Peak 1 (r.nm)	Intensity (%)	Peak 2 (r.nm)	Intensity (%)	Peak 3 (r.nm)	Intensity (%)
NS	8,284	75,2	49,02	23,6	2195	1,2
NSFA2	11,1	92,7	880,7	7,3	0	0
NSFA4	11,68	80,7	180	18,1	2086	1,2

DLS was used by several authors to determine the hydrodynamic radius of NS and NSF samples in order to verify the existence of the increase in particles with functionalization [[27]; [51]; [53]; [54]; [40]]. According to Martins [5] this increase in particle size is provided by the binding of functional groups on the surface of the NS and may vary according to the level of functionalization. The samples functionalized with aminosilanes followed the pattern of increasing in size as the APTES content increased, which is in agreement with Gu's research. *et al.* [13] and Martins [5]. The DLS results seem to show that the functionalization of the NS particles occurred as expected.

In the TGA test, it was possible to verify the mass loss of the samples as a function of temperature. The results are presented in Table 6. It was noted that the NS sample showed the lowest total mass loss (7.9%) among the analyzed samples. The NSF samples had increasing total mass losses as the functionalization content increased, with the NSFA4 sample having a much higher total mass loss than the other samples (21.7%).

Table 6: Localized mass losses and total samples.

Sample	Mass Loss	
	Entre 300°C e 800° C	Total
NS	1,7%	7,9%
NSFA2	3,4%	10,6%
NSFA4	5,0%	21,7%

According to Rong *et al* [3] the loss of mass between 300°C and 800°C observed in the TGA test may be due to the separation of the coupling agent grafted onto the surface of the NS particles. According to their research, the NSF mass loss rate between 300°C and 800°C can be used to approximate the engraftment rate of the coupling agent.

As can be seen, the mass loss increases with the increase in the functionalization content, demonstrating that the NSFA4 sample with the highest APTES content has the highest rate of grafted material on the NS surface. The result of the TGA test is in line with the results of the DLS test performed on the NS and NSF samples, as NSFA4 was the sample that presented the largest hydrodynamic radius, confirming that it is the sample with the highest number of APTES coupled to the surface of the NS.

3.2 MECHANICAL AND MICROSTRUCTURAL PROPERTIES OF PASTES AND MORTARS

3.2.1. Compressive strength

Figure 3 shows the compressive strength results of Portland cement mortars at 1, 3, 7 and 28 days of hydration.

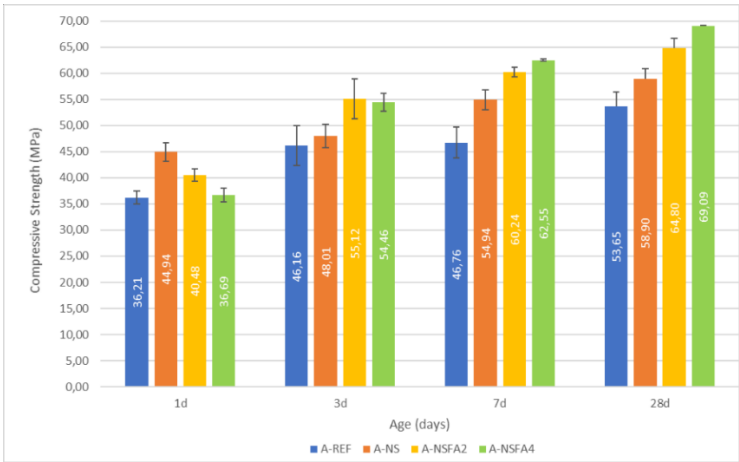

Figure 3: Compressive strength of mortars at 1, 3, 7 and 28 days.

Analyzing Figure 3, it is possible to observe that with 1 day of hydration, the A-NS mortar presented the highest average resistance (44.94MPa), corroborating the literature [[24]; [57]; [4]; [5]], with a resistance gain of 24.01% compared to A-REF. According to the literature, this resistance gain at initial ages in mortars with NS is quite characteristic and can be attributed to the effect of nucleation sites, filling effect and pozzolanic reactions. At the same age, when analyzing the mortars with NSF, it is possible to observe that A-NSFA4 (36.69MPa) presented the same strength as A-REF (36.21MPa), and A-NSFA2 exhibited a higher strength than A-REF by approximately 12%.

At 3 days of hydration, there is an expressive gain in resistance of mortars with NSF compared to the results presented with 1 day of hydration. The greatest increase in resistance between the NSF's was noticed in A-NSFA4 (54.46%), followed by A-NSFA2 (36.18%), showing that the APTES/NS volume ratio can influence the effect of NSF on the materials cementitious. After 3 days of hydration, it is possible to observe that mortars with NSF have superior resistance to mortars with NS, which is in line with researches already carried out by Vasconcellos [4] and Martins [5], who found a delay in the induction time of past containing NSF.

At 7 days, it was possible to observe that, as well as at 3 days of hydration, the resistance of all mortars with NSF continued to be higher than A-REF and A-NS. A-NSFA4 stands out, which had a resistance gain of 14.85% compared to the result achieved after 3 days of hydration, being the mortar that achieved the highest resistance among all samples at 7 days of hydration, although its resistance was slightly higher than that achieved by A-NSFA2 (60.24MPa). A-NSFA4 had a resistance gain of 33.77% when compared to A-REF at the same age, followed by A-NSFA2 (28.83%). Note that the higher the APTES content used in the functionalization of the NS, the greater the resistance achieved.

The compressive strength results of mortars with NSF at 28 days continued to be higher than the compressive strength results of A-REF and A-NS, as expected. The compressive strength of A-NS was superior to A-REF by 9.79%. The compressive strength results obtained by Martins [5] show that although NS provides a gain in mechanical performance at the initial ages, at 28 days this initial gain

does not have the same effect, probably due to autogenous retraction and the formation of the layer of C-S-H on the clinker surface, as also observed by other authors. [[24]; [29]; [30]; [4]]. When compared with A-NS, there is a resistance gain of 10% for A-NSFA2 and 17.29% for A-NSFA4.

3.2.2. Mercury intrusion porosimetry (MIP)

The mercury intrusion porosimetry (MIP) test aimed to evaluate the porous structure of cement pastes after 28 days of hydration. Figure 4 presents the results of the volume of mercury intruded in the analyzed samples. As can be observed in Figure 4, there was a refinement of the porous structure of the P-NS pastes and the P-NSFA2 and P-NSFA4 pastes compared to the P-REF paste.

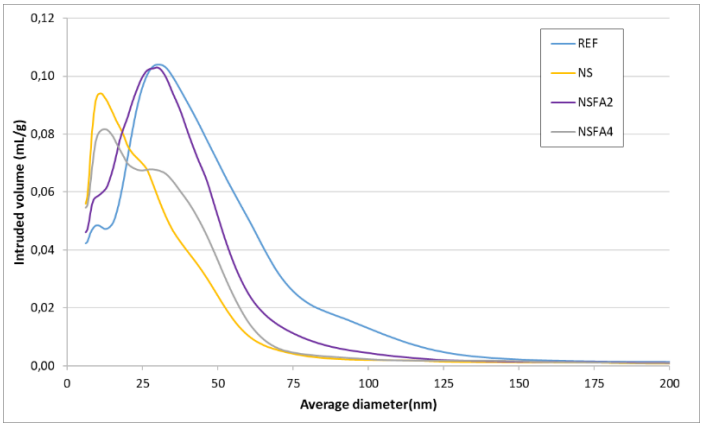

Figure 4: Volume of mercury intruded in the pastes at 28 days.

The results obtained for the P-NS sample are in accordance with the reference literature [[24]; [57]; [30]; [5]]. According to the literature, the pozzolanic activity of NS exerts a significant influence on the microstructure of cement-based materials, leading to a refinement in the material's pore structure. Wu et al. [60] compared the effects of different dosages of NS on the pore structure of high-strength concrete and observed the influence of the percentage of cement replacement by NS on porosity. They found that high replacement levels result in material agglomeration, leading to reduced paste fluidity and increased porosity. This occurs because material agglomeration limits the filling effect of NS.

Figure 5 presents the results of the accumulated volume of intruded mercury, which is related to the total porosity of the pastes. Analyzing Figure 5, it was noted that the total porosity among the pastes varied, with samples P-NS and P-NSFA4 showing the smallest accumulated intruded volume. It was observed that the addition of NS and NSF led to a reduction in total porosity, total intruded volume, and average diameter when compared to the reference mortar. The results obtained show that the incorporation of NS and NSF improves the porous structure of the pastes.

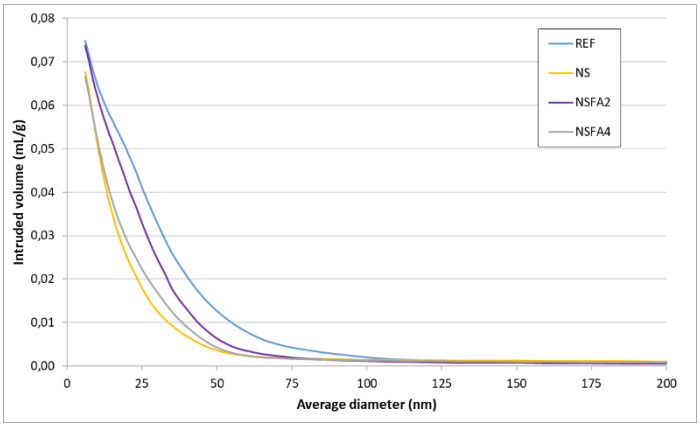

Figure 5 - Volume of mercury accumulated in the pastes at 28 days.

Table 7 presents a summary of the results found in the MIP test. It was observed that the incorporation of NS and NSF reduced the percentage of large and medium capillary pores, corroborating with the findings from Vasconcellos et al. [6] research.

Table 7 - Total porosity and volume of intruded mercury

Past	Total Intruded Volume (mL/g)	Total porosity (%)	Average pore diameter (nm)	Intruded mercury volume (mL/g)			
				Large capillary (10.000-50nm)		Medium capillary (50-10nm)	
				(mL/g)	(%) in relation to REF	(mL/g)	(%) in relation to REF
P-REF	0,0748	12,75	20,1	0,3979	100%	1,7762	100%
P-NS	0,0676	11,69	14,3	0,0980	25%	1,6395	92%
P-NSFA2	0,0737	12,55	17,8	0,1984	50%	1,8925	107%
P-NSFA4	0,0666	11,4	15,3	0,1358	34%	1,6463	93%

According to the literature [37], [65], [6], the reduction in pore size and total porosity when NS and NSF are incorporated into cementitious materials is due to the nucleation effect, the high reactivity of NS and NSF, and the pore-filling effect caused by the formation of additional C-S-H through the pozzolanic reaction. This pozzolanic reaction leads to a higher polymerization of the C-S-H chains, contributing to densification and compactness of the microstructure [[63]]. Vasconcellos et al. [6] research shows that the incorporation of NSF leads to a reduction in pore size and total porosity due to better dispersion caused by the amino silane groups. Similar results were observed in other research studies, [2], [27], and [67]. According to Mindess et al. [68], the reduction in porosity contributes to an increase in the mechanical performance and durability of cementitious materials.

IV. CONCLUSIONS

This article evaluated the effect of NSF with aminosilanes on the mechanical properties and microstructure of cementitious materials. The APTES/NS volume ratios used for NS functionalization were 2:60 (NSFA2) and 4:60 (NSFA4). Based on the experimental results in this work, the following conclusions can be drawn:

Through the presented results of DLS tests (an increase of the hydrodynamic radius), and ATG (an increase of the loss of mass), it was verified that the method used for functionalization of the NS with aminosilanes was effective in grafting the functional groups in different contents in the surface of the studied NS. It was verified that the hydrodynamic radius and the loss of mass of the samples get bigger with the increase of the functionalization content, demonstrating that the NSFA4 sample with the highest APTES content, presents the highest rate of grafted material on the surface of the NS.

The results of the compressive strength test of the mortars at 1, 3, 7 and 28 days of hydration in the mortars show that the extension of the induction period causes the mortars with NSF a delay in the resistance gain in initial ages. However, after 3 days of hydration the mortars with NSF already present resistance to compression superior to the samples A-NS and A-REF. The development of resistance to compression at 28 days of the A-NSFA4 sample was about 28.78% greater than the A-REF sample and about 17.29% greater than the A-NS, corroborating the results of Martins (2022), showing that the APTES content of 4mL seems to be the most appropriate for NS functionalization.

The MIP results show that, in general, the additions of NS and NSF lead to a decrease in total porosity, total intruded volume and average diameter, in relation to the reference mortar. This reduction in porosity contributes to increase the mechanical performance and durability of cementitious materials.

The variation in the proportion of APTES used to functionalize the NS caused changes in the hydration kinetics, CH content, pore size distribution of the pastes, and also altered the compressive strength of the Portland cement mortars. Therefore, it is concluded that the functionalization of the NS with different levels of aminosilane has the potential to be used in high-performance concretes. However,

despite the results presented, further studies are needed to better understand the behavior of the NS in cementitious media.

REFERENCES

[1]. Fernandez, JM; Duran, A.; Navarro-Blasco I.; Lanas, J.; Sirera, R.; Alvarez, JI. Influence of nanosilica and a polycarboxylate ether superplasticizer on the performance of lime mortars. Cement and Concrete Research, Volume 43, 2013, Pages 12-24, ISSN 0008-8846. https://doi.org/10.1016/j.cemconres.2012.10.007.

[2]. Feng, Pan; Chang, Honglei; Liu, Xin; Ye, Shaoxiong; Shu, Xin; Ran, Qianping. The significance of dispersion of nano-SiO2 on early age hydration of cement pastes. Materials & Design, Volume 186, 2020, 108320, ISSN 0264-1275. https://doi.org/10.1016/j.matdes.2019.108320.

[3]. Rong, Z.; Zhao, M.; Wang, Y. Effects of Modified Nano-SiO2 Particles on Properties of High-Performance Cement-Based Composites. Materials 2020, 13, 646. https://doi.org/10.3390/ma13030646.

[4]. Vasconcellos, J.S. (2021). Microstructure of Portland cement pastes with the Incorporation of Functionalized Nanosilica with Amine Groups. Doctoral Thesis in Structures and Civil Construction, Publication E.TD – 08A/21, Department of Civil and Environmental Engineering, University of Brasília, Brasília, DF, 248p.

[5]. Martins, G.L.O. (2022). Microstructure of Portland cement pastes containing functionalized nanosilica with different proportions of aminosilane. Doctoral Thesis in Structures and Civil Construction, Publication E.DM-XXA/22, Department of Civil and Environmental Engineering, University of Brasília, Brasília, DF, 189p.

[6]. Vasconcellos, Julliana Simas; Fraga, Yuri Sotero Bomfim; Rêgo, João Henrique da Silva; Sartoratto, Patrícia Pommé Confessori; Rojas, Moisés Cold. Hydration, mechanical performance and porosity of Portland cement pastes with functionalized nanosilica with APTES, Developments in the Built Environment, Volume 14, 2023, 100157, ISSN 2666-1659, https://doi.org/10.1016/j.dibe.2023.100157.

[7]. Senff, Luciano; Labrincha, João A., Ferreira, Victor M., Hotza, Dachamir, Repette, Wellington L. Effect of nano-silica on rheology and fresh properties of cement pastes and mortars, Construction and Building Materials, Volume 23, Issue 7, 2009, Pages 2487-2491, ISSN 0950-0618, https://doi.org/10.1016/j.conbuildmat.2009.02.005.

[8]. Madani H, Bagheri A, Parhizkar T. The pozzolanic reactivity of monodispersed nanosilica hydrosols and their influence on the hydration characteristics of Portland cement. One Hundred Concr Res. 2012;42(12):1563–570. https://doi.org/10.1016/j.cemconres.2012.09.004.

[9]. Li, L.G; Huang, Z.H; Zhu, J.; Kwan, A.K.H; Chen, H.Y. Synergistic effect of microsilica and nano-silica on strength and microstructure of mortar. Construction and Building Materials, vol. 140, p. 229-238, 2017.

[10]. Mendes, T.M; Repette, WL. Effect of nano-silica on Portland cement matrix. Rev. IBRACON Struct. Mater. 12 (06), Nov-Dec 2019. https://doi.org/10.1590/S1983-41952019000600009.

[11]. Singh, L.P; Karade, S.R; Bhattacharyya, S.K; Yousuf, M.M; Ahalawat, S. Beneficial role of nanosilica in cement based materials – A review. Construction and Building Materials, vol. 47, p. 1069-1077, 2013.

[12]. Schmalz, Rosana. Durability of mortars subjected to sulfate attack: effect of adding nanosilica. Thesis (Master's degree). Federal University of São Carlos. São Carlos – SP, 2018.

[13]. Gu, Y., Ran, Q., She, W., & Liu, J. Modifying Cement Hydration with NS@PCE Core-Shell Nanoparticles. Advances in Materials Science and Engineering, 2017(1), 1–13. 2017.

[14]. Fang, Y.I; Wang, Jialai; M.A, Haibin; Wang, Liang; Qian, Xin; Qiao, Pizhong. Performance enhancement of silica fume blended mortars using bio-functionalized nano-silica. Construction and Building Materials, Volume 312, 2021, 125467, ISSN 0950-0618. https://doi.org/10.1016/j.conbuildmat.2021.125467.

[15]. Singh, L.P.; Agarwal S.K, Bhattacharyya S.K, Sharma U, Ahalawat, S. Preparation of Silica Nanoparticles and its Beneficial Role in Cementitious Materials. Nanomaterials and Nanotechnology. 2011;1. https://doi.org/doi: 10.5772/50950 .

[16]. Durgun, Muhammed Yasin; Atahan, Hakan Nuri. Rheological and fresh properties of reduced fine content self-compacting concretes produced with different particle sizes of nano SiO2. Construction and Building Materials, Volume 142, 2017, Pages 431-443, ISSN 0950-0618. https://doi.org/10.1016/j.conbuildmat.2017.03.098.

[17]. Ren, Chunrong et al. Preparation and properties of nanosilica-doped polycarboxylate superplasticizer. Construction and Building Materials, vol. 252, p. 119037, 2020: https://doi.org/10.1016/j.conbuildmat.2020.119037.

[18]. Said, A.M; Zeidan, M.S; Bassuoni, M.T; Tian, Y. Properties of concrete incorporating nano-silica. Construction and Building Materials, vol. 36, no. 1, p. 838-844, 2012.

[19]. Balapour, Mohammad; Joshaghani, Alireza; Althoey, Fadi. Nano-SiO2 contribution to mechanical, durability, fresh and microstructural characteristics of concrete: A review. Construction and Building Materials, vol. 181, p. 27–41, 2018. https://doi.org/10.1016/j.conbuildmat.2018.05.266.

[20]. Lim, Seungmin; Lee, Han Seung; Kawashima, Shiho. Pore structure refinement of cement paste incorporating nanosilica: Study with dual beam scanning electron microscopy/focused ion beam (SEM/FIB). Materials Characterization, v. 145, no. August, p. 323–328, 2018. https://doi.org/10.1016/j.matchar.2018.08.045.

[21]. Martins, G.L.O; Fraga, Y.S.B; Vasconcellos, J.S; Rêgo, J.H.S Synthesis and characterization of functionalized nanosilica for cementitious composites: review. Journal of Nanoparticle Research, v. 22, p. 1-10, 2020.

[22]. Thomas, Jeffrey J., Biernacki, Joseph J., Bullard, Jeffrey W., Bishnoi, Shashank, Dolado, Jorge S., Scherer, George W., Luttge, Andreas. Modeling and simulation of cement hydration kinetics and microstructure development, Cement and Concrete Research, Volume 41, Issue 12, 2011, Pages 1257-1278, ISSN 0008-8846, https://doi.org/10.1016/j.cemconres.2010.10. 004.

[23]. Hou, Peng-Kun; Kawashima, Shiho; Wang Ke-Jin; Corr, David J.; Qian, Jue-Shi; Shah, Surendra P. Effects of colloidal nanosilica on rheological and mechanical properties of fly ash–cement mortar. Cement and Concrete Composites, Volume 35, Issue 1, 2013, Pages 12-22, ISSN 0958-9465. https://doi.org/10.1016/j.cemconcomp.2012.08.027.

[24]. Andrade, D. da S.; Rêgo, J.H da S.; Morais, P.C; Lopes, An de M.; Rojas, M. F. Investigation of C-S-H in ternary cement pastes containing nanosilica and highly-reactive supplementary cementitious materials (SCMs): Microstructure and strength. Construction and Building Materials, vol. 198, p. 445–455, 2019.

[25]. Rathod, Nikesh Ganesh, Moharana, N.C, Parashar, S.K.S. Effect of nano-SiO2 on physical and electrical properties of PPC cement using complex impedance spectroscopy, Materials Today: Proceedings, Volume 5, Issue 1, Part 1, 2018, Pages 193-199 , ISSN 2214-7853, https://doi.org/10.1016/j.matpr.2017.11.071.

[26]. Meng, Tao, Hong, Yongpeng, Wei, Huadong, Xu, Qinglei. Effect of nano-SiO2 with different particle size on the hydration kinetics of cement, Thermochimica Acta, Volume 675, 2019, Pages 127-133, ISSN 0040-6031, https://doi.org/10.1016/j.tca.2019.03 . 013.

[27]. Liu, X.; Feng, P.; Shu, X.; Ran, Q. Effects of highly dispersed nano-SiO2 on the microstructure development of cement pastes. Materials and Structures/Materiaux et Constructions, v. 53, no. 1, p. 1–12, 2020.

[28]. Althoey, Fadi, Zaid, Osama, Martínez-García, Rebeca, Alshharari, Fahad, Ahmed, Mohd, Arbili, Mohamed M. Impact of Nano-silica on the hydration, strength, durability, and microstructural properties of concrete: A state-of -the-art review, Case Studies in Construction Materials, Volume 18, 2023, e01997, ISSN 2214-5095, https://doi.org/10.1016/j.cscm.2023.e01997.

[29]. Fraga, Yuri Sotero Bomfim; Martins, Gabriel Lima Oliveira; Rêgo, João Henrique da Silva. Influence of functionalized nanosilica with different functional groups in the properties of cementitious composites : A review. Research, Society and Development, v. 10, no. 8, e27719817349, 2021 (CC BY 4.0) | ISSN 2525-3409 | DOI: http://dx.doi.org/10.33448/rsd-v10i8.17349.

[30]. Sousa, Matheus Ian Castro; Rêgo, João Henrique da Silva. Effect of nanosilica/metakaolin ratio on the calcium alumina silicate hydrate (CASH) formed in ternary cement pastes, Journal of Building Engineering, Volume 38, 2021, 102226, ISSN 2352-7102, https://doi.org/10.1016/j. jobe.2021.102226.

[31]. Collodetti, Giovana; Gleize, Philippe J.P; Monteiro, Paulo J.M. Exploring the potential of siloxane surface modified nano-SiO2 to improve the Portland cement pastes hydration properties. Construction and Building Materials, Volume 54, 2014, Pages 99-105, ISSN 0950-0618. https://doi.org/10.1016/j.conbuildmat.2013.12.028.

[32]. Monasterio, Manuel et al. Effect of addition of silica- and amine functionalized silica-nanoparticles on the microstructure of calcium silicate hydrate (C-S-H) gel. Journal of Colloid and Interface Science, v. 450, p. 109–118, 2015. http://dx.doi.org/10.1016/j.jcis.2015.02.066.

[33]. Pérez, G.; Gaitero, J.J; et al. Characterization of cement pastes with innovative self-healing system based on epoxy-amine adhesive. Cement and Concrete Composites, v. 60, p. 55–64, 2015. http://dx.doi.org/10.1016/j.cemconcomp.2015.03.010.

[34]. Gu, Yue et al. Synthesis of nanoSiO2@PCE core-shell nanoparticles and its effect on cement hydration at early age. Construction and Building Materials, vol. 114, p. 673–680, 2016. http://dx.doi.org/10.1016/j.conbuildmat.2016.03.093.

[35]. Gu, Yue; Wei, Zhenhua; et al. Characterizing cement paste containing SRA modified nanoSiO2 and evaluating its strength development and shrinkage behavior. Cement and Concrete Composites, v. 75, p. 30–37, 2017. http://dx.doi.org/10.1016/j.cemconcomp.2016.11.001.

[36]. Huang, Chunlong; Wang, Dongmin. Surface Modification of Nano-SiO2 Particles with Polycarboxylate Ether-Based Superplasticizer under Microwave Irradiation. ChemistrySelect, v. 2, no. 29, p. 9349–9354, 2017.

[37]. Gu, Yue et al. Effects and mechanisms of surface-treatment of cementitious materials with nanoSiO2@PCE core-shell nanoparticles. Construction and Building Materials, vol. 166, p. 12–22, 2018. https://doi.org/10.1016/j.conbuildmat.2018.01.082.

[38]. Azevedo, Nagilla Huerb de; Gleize, Philippe J.P. Effect of silicon carbide nanohiskers on hydration and mechanical properties of a Portland cement paste. Construction and Building Materials, vol. 169, p. 388–395, 2018. https://doi.org/10.1016/j.conbuildmat.2018.02.185.

[39]. Vasconcellos, J.S; Martins, G.L.O; Almeida Ribeiro Oliveira, G. de; Lião, L.M; Silva Rêgo, J.H da; Sartoratto, P.P.C. Effect of amine functionalized nanosilica on the cement hydration and on the physical-mechanical properties of Portland cement pastes. Journal of Nanoparticle Research, v. 22, no. 8, 2020.

[40]. ABNT - Brazilian Association of Technical Standards. NBR 16697: Portland Cement - Requirements. Rio de Janeiro, 2018.

[41]. ABNT - Brazilian Association of Technical Standards. NBR 11768-1: Chemical additives for Portland cement concrete - Part 1: Requirements. Rio de Janeiro, 2019.

[42]. Sun, J.; Shi, H.; Qian, B.; Xu, Z., Li, W.; Shen, X. Effects of synthetic C-S-H/PCE nanocomposites on early cement hydration. Construction and Building Materials, 140, 282–292. 2017.

[43]. Huang, Chunlong et al. Potential Effect of Surface Modified Nano-SiO2 with PDDA on the Cement Paste Early Hydration. ChemistrySelect, v. 5, no. 11, p. 3159–3163, 2020.

[44]. ABNT - Brazilian Association of Technical Standards. NBR 7215: Portland Cement - Determination of compressive strength of cylindrical specimens. Rio de Janeiro, 2006.

[45]. ABNT - Brazilian Association of Technical Standards. NBR 16606: Portland Cement - Determination of normal consistency paste. Rio de Janeiro, 2018.

[46]. Ordóñez, S.T.L. Mitigation of autogenous shrinkage in high strength microconcrete with addition of superabsorbent polymers and shrinkage reducing additive. 2013. 160 f. Dissertation (Master in Structures and Civil Construction) - University of Brasília, Brasília, 2013.

[47]. Manzano, Manuel Alejandro Rojas. Experimental study of high strength cementitious materials modified with superabsorbent polymers (PSAs) as internal curing agents. 2016. University of Brasília, 2016. https://repositorio.unb.br/handle/10482/22140.

[48]. Scrivener, K.; Snellings, R.; Lohenbach, B. A practical guide to microstructural analysis of cementitious materials. CRC PTRESS, 2016.

[49]. Alonso-Domínguez, D.; Álvarez-Serano, I.; Reyes, E.; Moragues, A. New mortars fabricated by electrostatic dry deposition of nano and microsilica additions: Enhanced properties, Construction and Building Materials, Volume 135, 2017, Pages 186-193, ISSN 0950-0618, https://doi.org/10.1016/ j.conbuildmat.2017.01.011.

[50]. Boul, Peter J; Shanmugam, Sivaprakash; Johnson, Kenneth D. Nanosilica functionalized to switch from dormant to active for gas migration mitigation in Portland cement. n. June, p. 1–13, 2021.

[51]. Sargam, Yogiraj; Wang, Kejin. Influence of dispersants and dispersion on properties of nanosilica modified cement-based materials. Cement and Concrete Composites, v. 118, no. February, p. 103969, 2021. Available at: https://doi.org/10.1016/j.cemconcomp.2021.103969 .

[52]. Sousa, Ionara Pereira da Silva. Obtaining functionalized nanosilica for use as an additive in cement mixtures. [Sl: sn], 2017.

[53]. Rêgo, J.H.S; Rojas, M.F; Terrades, A.M; Fernandez-Carrasco, L.; Morales, E.R; Rojas, M.I.S (2019). Effect of partial substitution of highly reactive mineral additions by nanosilica in cement pastes. J. Mater. Civ. Eng., v.31(1). 2019.

[54]. Fraga, Yuri Sotero Bomfim; Rêgo, João Henrique da Silva; Capuzzo, Valdirene Maria Silva; Andrade, Daniel da Silva. Ultrasonication effect of silica fume and colloidal nanosilica on cement pastes. Revista Matéria, ISSN 1517-7076 articles e-12847, 2020, V 25, nº4. https://doi.org/10.1590/S1517-707620200004.1147.

[55]. Frias, M.; de la Villa, R.V; Garcia, R.; Rodriguez, O.; Fernandez Carrasco, L.; Martínez-Ramirez, S. Carbonation-induced mineralogical changes in coal mining waste blended cement pastes and their influence on mechanical and microporosity properties. Minerals, v. 8, p. 169-185. 2018.

[56]. Monteagudo, S.M, Moragues, A., Gálvez, J.C, Casati, M.J, Reyes, E. The degree of hydration assessment of blended cement pastes by differential thermal and thermogravimetric analysis. Morphological evolution of the solid phases, Thermochimica Acta, Volume 592, 2014, Pages 37-51, ISSN 0040-6031, https://doi.org/10.1016/j.tca.2014.08.008.

[57]. Haruehansapong, Sattawat, Pulngern, Tawich, Chucheepsakul, Somchai. Effect of the particle size of nanosilica on the compressive strength and the optimum replacement content of cement mortar containing nano-SiO2, Construction and Building Materials, Volume 50, 2014, Pages 471-477, ISSN 0950-0618, https://doi. org/10.1016/j.conbuildmat.2013.10.002.

[58]. Singh, L.P, S.K, Bhattacharyya, Shah, S.P, G., Mishra, Sharma, U. Studies on early stage hydration of tricalcium silicate incorporating silica nanoparticles: Part II, Construction and Building Materials, Volume 102, Part 1, 2016, Pages 943-949, ISSN 0950-0618, https://doi.org/10.1016/j.conbuildmat.2015.05.084.

[59]. Khaloo, Alireza, Mobini, Mohammad Hossein, Hosseini, Payam. Influence of different types of nano-SiO2 particles on properties of high-performance concrete, Construction and Building Materials, Volume 113, 2016, Pages 188-201, ISSN 0950-0618, https://doi.org/10.1016/j.conbuildmat .2016.03.041.

[60]. Wu, Zemei, Shi, Caijun, Khayat, K.H, Wan, Shu. Effects of different nanomaterials on hardening and performance of ultra-high strength concrete (UHSC), Cement and Concrete Composites, Volume 70, 2016, Pages 24-34, ISSN 0958-9465, https://doi.org/10.1016/j. cemconcomp.2016.03.003.

[61]. Fu, Q., Zhao, X., Zhang, Z., et al. "Effects of nanosilica on microstructure and durability of cement-based materials", Powder Technology, v. 404, pp. 117447, 2022. doi: http://dx.doi.org/10.1016/j. powtec.2022.117447.

[62]. Land, G., Stephan, D. The influence of nano-silica on the hydration of ordinary Portland cement, J. Mater. science, 47 (2012), pp. 1011-1017, 10.1007/s10853-011-5881-1 .

[63]. Singh, L.P, S.K, Bhattacharyya, Shah, S.P, G., Mishra, Ahalawat, S., Sharma, U. Studies on early stage hydration of tricalcium silicate incorporating silica nanoparticles: Part I, Construction and Building Materials, Volume 74, 2015 , Pages 278-286 , ISSN 0950-0618, https://doi.org/10.1016/j.conbuildmat.2014.08.046 .

[64]. Zhang, Zhigang; L.I, Zhipeng; H.E, Jialuo; Shi, Xianming. High-strength engineered cementitious composites with nanosilica incorporated: Mechanical performance and autogenous self-healing behavior, Cement and Concrete Composites, Volume 135, 2023, 104837, ISSN 0958-9465, https://doi.org/10.1016/j.cemconcomp.2022.104837.

[65]. Kshirsagar, A. D.; Mahulikar, P. P. Microwave-assisted synthesis of poly(glycidylazide-co-tetrahydrofuran). Polymer Bulletin, v. 74, n. 5, p. 1727–1742. 2017.

[66]. Xu, Zhenhai; Zhou, Zonghui; Du, Peng; Cheng, Xin. Effects of nano-silica on hydration properties of tricalcium silicate. Construction and Building Materials, Volume 125, 2016, Pages 1169-1177, ISSN 0950-0618. https://doi.org/10.1016/j.conbuildmat.2016.09.003

[67]. Rupasinghe, M.; San Nicolas, R.; Mendis, P.; M. Sofi, T. Ngo. Investigation of strength and hydration characteristics in nanosilica incorporated cement paste. Cement and Concrete Composites, v. 80, 2017.

[68]. Mindess, S.; Young, J.F; Darwin, D. Developments in the Formulation and Reinforcement of Concrete, Concrete (second ed.) (2002), New Jersey.

AUTHORS

Andréia de Paula is a master's student in Structures and Civil Construction at the University of Brasília (UnB/Brazil). She received her degree in Civil Engineering from the Federal University of Juiz de Fora (UFJF/Brazil) in 2003. Her research interests include concrete microstructure, nanomaterials and high-performance concrete.

Yuri Sotero Bomfim Fraga is a professor of civil engineering at the Federal University of Acre (UFAC/Brazil). He received his master´s degree in Structures and Civil Construction from the University of Brasília (UnB/Brazil) in 2019. His research interests include concrete microstructure, nanomaterials and high-performance concrete.

João Henrique da Silva Rêgo is a professor of civil engineering at the University of Brasília (UnB/Brazil). He received his PhD in Structures and Civil Construction from the UnB/Brazil in 2004. His research interests include Portland cement, agro-industrial waste, concrete microstructure, microstructural analysis techniques, nanosilica, nanotechnology of cementitious materials.

Maria José de Souza Serafim is a researcher in Civil Engeneering at the University of Brasília (UnB/Brazil). She received her PhD in Analytical and Inorganic Chemistry at the University of Brasília (UnB/Brazil) in 2005. Her research interests include nanosilica functionalization and application in concrets, properties and microstructural characterization of these cementitious materials.